ISSN 1068-3666, Journal of Friction and Wear, 2017, Vol. 38, No. 5, pp. 401–406. © Allerton Press, Inc., 2017.
Original Russian Text © R.I. Nepershin, 2017, published in Trenie i Iznos, 2017, Vol. 38, No. 5, pp. 475–482.

Plastic Deformation of the Surface Layer's Microroughness by a Sliding Tool with Strong Contact Friction

R. I. Nepershin

Moscow State Technological University STANKIN, Moscow, 127994 Russia

e-mail: nepershin_ri@rambler.ru

Received June 30, 2016

Abstract—The plastic deformation of the discrete contacts of a tool with a circular-arc and an inclined profile with the periodical microroughnesses of the metallic part's surface layer is modeled. The plane deformation theory of a perfectly plastic body is used. The plastic deformation process of the surface layer's microroughnesses by a sliding tool with Prandtl's high contact friction in which the plastic shear occurs in the direction of the slide of the tool, with the microroughnesses' depressions being filled and a decrease of the surface roughness, is studied.

Keywords: microroughness, repetitive form, plastic deformation, sliding tool, contact friction, perfect plasticity, plane deformation

DOI: 10.3103/S1068366617050105

INTRODUCTION

The surface plastic deformation (SPD) of a rough surface after shaving the workpiece by a high-performance cutting tool allows us to reduce the number of time-consuming additional transitions aimed at improving the surface finish of the processed part [1, 2]. The surface roughness depends on the shape of the cutting tool and the technological cutting method. An evaluation of the roughness of the plane's surface with peripheral milling is presented in [3]. The tool for the SPD should be hard and wear resistant with a high manufacturing accuracy level and surface finish by an order of magnitude exceeding the roughness of the processed part. Moreover, the plasma spraying technology of wear-resistant coatings [4–6] whose application allows us to regulate the tool's contact friction with the plastically deformed microroughnesses of the processed surface is effective.

With the traditional technological modes, SPD penetrates at a thickness exceeding the surface roughness. Stationary process modeling of an SPD based on the plane deformation theory of a perfectly plastic body [7] with the sliding and swinging of the tool is given in the papers [8, 9].

Modeling the SPD process by a sliding tool according to the plane deformation theory of a perfectly plastic body with discrete contacts with periodic protrusions of a rough surface is presented in [9]. The mechanics of the protrusions of a rough surface on contact with the tool under insignificant friction have been considered. In this case, the depressions are filled and the surface roughness decreases due to the yielding of the right and the left edges of the deformed protrusion.

The reduction of the initial microroughness and the depressions' residual depth are limited by the maximum permissible pressure of the sliding tool; if the permissible limit is exceeded, the plastic deformation penetrates into the depth of the processed part's surface layer. The maximum permissible pressure and the processed part's final roughness are determined by the pressure of a sliding flat die on the plastic half space taking Prandtl's contact friction into account.

The plastic deformation of the discrete protrusions of the microroughnesses of rough surfaces by a hard tool with a circular arc and an inclined profile with Prandtl's high contact friction values has been modeled in this study. In this case the shearing mechanism of the microroughness protrusions' plastic deformation with a one-way plastic yielding in the direction that the tool is sliding prevails. This results in a decrease of the residual depth of the depressions of the microroughness and the roughness of the processed surface compared to the deformation by a sliding tool with low contact friction [9].

THE AIM OF THE STUDY

We aim to develop a plastic deformation model of the discrete contacts of a tool with a circular arc and an inclined profile with periodic microroughnesses of the surface layer of the metallic part.

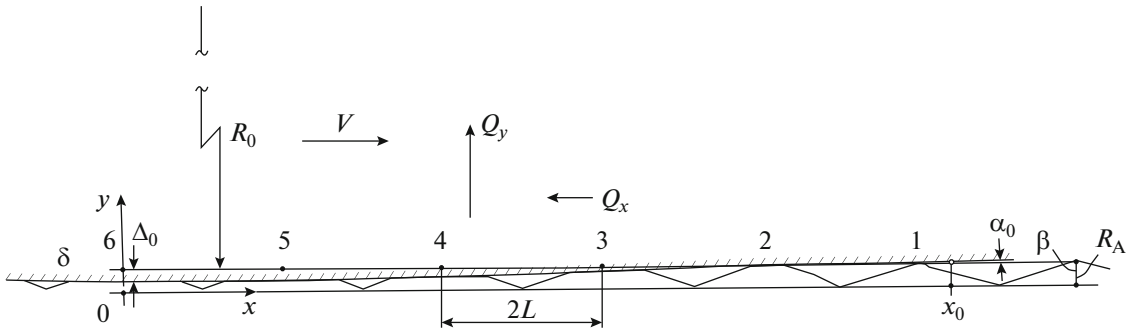

Fig. 1. Plastic deformation of rough surface by sliding tool. 1–6 are the numbers of deformed protrusions.

DEVELOPMENT OF THE MODEL

Main Equations

A plastic deformation of a rough surface's protrusions with discrete contacts with a hard sliding tool is shown in Fig. 1. The tool's surface roughness is small compared to the processed part's roughness. The rough surface's periodic form with the straight-line boundaries of the protrusions and depressions is assumed.

The projections' height relative to the depressions is assumed as the characteristic dimension $R_A = 1$. The nondimensional half-length $L = \tan\beta$ between the protrusions and depressions is determined by the half apex angle β of the protrusions and depressions. The protrusions' discrete plastic deformation occurs with the horizontal sliding of the tool relative to the processed surface at speed V with a vertical shift Δ_0 of the tool's lower point with the circular-arc profile with radius R_0 or the linear profile with the angle of inclination α_0 in relation to the horizontal axis in Fig. 1.

In the case when the tool has a circular-arc profile, the discrete contacts' zone is determined by the critical angle α_0 at the intersection of the tool's boundary with the lines of the protrusions. With $R_0 \gg 1$, the angle α_0 and the digital number of contacts N_c are determined by formulas [9]:

$$\alpha_0 = \sqrt{2\frac{\Delta_0}{R_0}}, \quad (1)$$

$$N_c = \text{int}(R_0\alpha_0/2L) + 1. \quad (2)$$

With the sliding of the tool, the protrusion spaced apart from the origin of coordinates O at the distance $2L(N_c - 1)$ comes into contact first. The plastic deformation ends at the protrusion with number N_c with $x = 0$. The distances x_i, the angles of descent to the tool's circular-arc profile α_i, and the compression ratios in the height Δ_i of the deformed protrusions with numbers $i = 1, 2, ..., N_c$ on the assumption $\alpha_i \ll 1$ are determined by the formulas

$$x_i = 2L(N_c - i), \quad \alpha_i = x_i/R_0,$$
$$\Delta_i = \Delta_0 - \tfrac{1}{2}R_0\alpha_i^2, \quad i = 1, 2, \ldots, N_c. \quad (3)$$

Due to the smallness of the angles α_i, the tool's circular-arc profile boundaries at the contact with the protrusions i are assumed as straight inclination angles α_i to the x axis.

In the case of the tool's linear profile, the specified inclination angles α_0, and shift Δ_0 of the profile's gage, the number of discrete contacts with the microroughness' deformed protrusions and the deformed protrusions' compression ratios Δ_i are determined by the formulas

$$N_c = \text{int}(\Delta_0\cot\alpha_0/2L) + 1, \quad \Delta_i = \Delta_0 - x_i\tan\alpha_0, \quad (4)$$

where the coordinates x_i of the deformed protrusions' apexes are determined by formula (3). On the profile's gage, $i = N_c$, $x \le 0$, and $\alpha = 0$.

The plastic yielding's stressed state and kinematics with a deformation of the protrusions are estimated according to the plane deformation theory of a perfectly plastic body [7], assuming the duplicated plastic invariable as the unit stress $2k = 1$, $k = \sigma_s/\sqrt{3}$, with provision for the material strengthening while evaluating the numerical values of the yield stress σ_s. At the tool's boundaries, Prandtl's friction stress is $\tau_c < 0.5$.

The plastic yielding of the deformed protrusions is determined by the sliding lines' equations ξ and η:

$$dy/dx = \tan\varphi \text{ for } \xi, \quad dy/dx = -\cot\varphi \text{ for } \eta, \quad (5)$$

where φ is the angle of descent towards the sliding line ξ with the x axis by the Hencky relations

$$\sigma - \varphi = \text{const along } \xi, \quad \sigma + \varphi = \text{const along } \eta \quad (6)$$

for the average stress σ and the angle φ, and the Geiringer relations for the velocities' projections V_ξ and V_η on a sliding line

$$dV_\xi - V_\eta d\varphi = 0 \text{ along } \xi, \quad dV_\eta + V_\eta d\varphi = 0 \text{ along } \eta. \quad (7)$$

The equations (5)–(7) are solved by the numerical method [10], while determining the sliding lines, stresses, and speed in a plastic region with the contact friction's boundary conditions τ_c of the zero equations of the normal and tangential stresses on a stress-free boundary and the velocity vector's normal component on the contact with the tool and on the rigid-plastic boundaries. The calculations are automated with the FORTRAN program with the graphic output on the display monitor and tables of the numeric values.

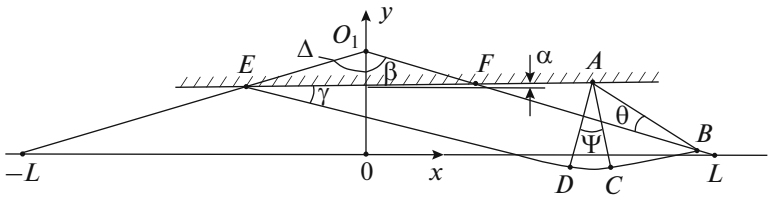

Fig. 2. Sliding lines at first deformation stage with $\alpha = 0.015$, $\beta = 1.279$, $\Delta = 1/3$, $\mu = 0.435$.

The First Stage of a Deformation

The sliding lines of the initial automodeling stage of the protrusions' plastic deformation by the sliding tool with the inclination angle α, the contact friction coefficient μ with the vertical shift Δ of the contact surface with respect to the apex of the protrusion's microroughness. The sliding lines and the velocity field due to the geometric similarity of the expanding plastic region do not depend on Δ.

With the tool's sliding, a nonsymmetrical deformation of the protrusion occurs with the material's protrusion on the inclined boundary AB at angle θ to the protrusion's right boundary. The stresses in the plastic region $ABCDE$ satisfying Eqs. (5) and (6) with the boundary condition $\sigma = -0.5$ on AB and the friction stress $\tau_c = \mu$ on AE are determined by the homogeneous stress state in zones ABC and ADE and the centered spiral fan with the spiral fan's angle ψ at point A. The normal pressure on the tool is determined by the formula

$$p = \psi + 0.5(1 + \sin 2\gamma), \quad \gamma = 0.5\arccos 2\mu. \qquad (8)$$

The equality of the areas of triangles O_1EF and ABF follows from the plastic incompressibility condition, resulting in a nonlinear relation for the angle θ in the form [10]

$$b\left[\cos\nu - \sqrt{2}\sin\gamma\sin\theta\right]^2 - \sin\theta\cos(\theta + \nu) = 0,$$
$$\nu = \alpha - \beta, \quad b = \frac{1}{4}\frac{\cos^2\alpha}{\sin^2\gamma}\frac{\left(\cot^2\beta - \tan^2\alpha\right)}{\cos\nu\cot\beta}. \qquad (9)$$

With small angles θ, the Eq. (9) possesses the solution

$$\theta = b\frac{\cos\nu}{1 + 2\sqrt{2}\sin\gamma}. \qquad (10)$$

The adjusted value θ is evaluated by solving Eq. (9) by Newton's method with the initial approximation (10). The contact boundary's length l_c and the angle ψ are calculated by the formulas

$$l_c = a\cos\nu[\cos\nu - \sqrt{2}\sin\gamma\sin\theta]^{-1}, \quad \nu = \alpha - \beta, \qquad (11)$$

$$a = 2\cot\beta\left[\left(\cot^2\beta - \tan^2\alpha\right)\cos\alpha\right]^{-1},$$
$$\psi = \beta + \gamma - (\pi/4 + \alpha + \theta). \qquad (12)$$

The load-bearing capacity of the rigid region of the wedge with the apex at point E results in the following inequality for the angle ψ:

$$\Psi \le \alpha + \beta + \gamma - \pi/4. \qquad (13)$$

Substituting ψ from (12) into (13) leads to the inequality $-(\alpha + \theta) \le \alpha$, which is realized with all the values of the problem parameters as $\theta > 0$.

The forces affecting the tool increase linearly proportionally to the shift Δ and are determined by the contact stresses

$$Q_x = l_c\Delta(p\sin\alpha + \mu\cos\alpha),$$
$$Q_y = l_c\Delta(p\cos\alpha - \mu\sin\alpha). \qquad (14)$$

With the high contact friction values $\mu \to 0.5$ and $\gamma \to 0$, the angle ψ, the pressure p, and the vertical force Q_y decrease with the increase of the horizontal force Q_x in comparison with the deformed protrusions of the tool with low contact friction μ.

The coordinates of points A, B, and E, defining the plastic region at the automodeling stage of the protrusion's deformation, are determined by the formulas

$$x_E = \Delta/(\tan\alpha - \cot\beta),$$
$$y_E = 1 - \Delta + x_E\tan\alpha, \quad \text{point } E, \qquad (15)$$

$$x_A = x_E + l_c\cos\alpha, \quad y_A = y_E + l_c\sin\alpha, \quad \text{point } A, \qquad (16)$$

$$x_B = x_A + \sqrt{2}l_c\cos\gamma\sin(\beta - \theta),$$
$$y_B = y_A - \sqrt{2}l_c\cos\gamma\cos(\beta - \theta), \quad \text{point } B. \qquad (17)$$

The automodeling stage of the protrusion's deformation ends when shifting point B into the lowest point of the depression in the roughness. The boundary shift Δ^* is determined by the equation γ_B^* with the substitution of y_A and y_E into the second formula (17) and l_c from formula (11):

$$\Delta^* = (\cos\alpha - \sin\alpha\tan\beta)/\zeta, \quad \zeta = \cos\alpha$$
$$+ 2\frac{\sqrt{2}\sin\gamma\cos(\beta - \alpha) - \sin\alpha}{(\tan\alpha + \cot\beta)\left(1 - \sqrt{2}\sin\gamma\sin\theta/\cos(\alpha - \beta)\right)}. \qquad (18)$$

The Second Stage of a Deformation

With $\Delta > \Delta^*$, the plastic yielding occurs in the depression on the right side of the roughness with the

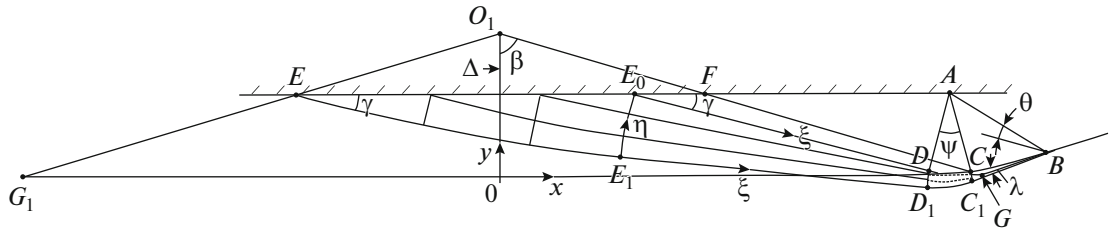

Fig. 3. Sliding lines at second deformation stage.

straight boundary AB, with the retention of the angles θ and ψ formed at the first stage of the deformation.

The sliding lines in the plastic region at the second stage of the deformation are shown in Fig. 3. The length l_c of the contact boundary AE is determined by the shift Δ and the equality of the area of triangle EFO_1 to the area of quadrangle $ABGF$ with the right depression of the microroughness being filled with the material.

$$2\Delta^2\cot\beta\Big/\left(\cot^2\beta - \tan^2\alpha\right) = \Delta^2\Big/(\tan\alpha + \cot\beta) - 2\tan\beta + x_A x_B(\tan\alpha - \cot\beta) + (x_A + x_B)(2 - \Delta). \quad (19)$$

The coordinates x_B of point B are related to the coordinate x_A of point A by a linear relation, which is determined by the intersection of the adjacent protrusion's left edge with the line passing through point A with the inclination angle θ towards the protrusion's right edge. Equation (19) is transformed into the form of a quadratic equation in relation to x_A, from which the value x_A is evaluated. The coordinates of point E are determined by the shift Δ by formulas (15) and the coordinate y_A is determined by the second formula (16). Then length l of the stress-free boundary AB,

$$l = [(x_A - x_B)^2 + (y_A - y_B)^2]^{1/2}, \quad (20)$$

and the length l_c of the contact boundary AE,

$$l_c = (x_A - x_E)/\cos\alpha, \quad (21)$$

are evaluated.

In the region $ABCDE_0$, the sliding lines are determined by the length l of the boundary AB, the contact friction μ, and the angle ψ of the centered fan of the sliding lines at point A. With an increase of the tool's shift Δ, the length l decreases when the right depression of the microroughness is filled. The length $l_0 = l/(\sqrt{2}\sin\gamma)$ of the interval AE_0 of the contact of the boundary with a constant pressure (8) decreases. The length $s = l_c - l_0$ of the interval EE_0 of the boundary contact is determined by the numerical evaluation of the sliding lines below ξ—the line $BCDE_0$ according to Eqs. (5) and (6) depending on angle λ of the centered fan of the sliding lines at point B. The angle λ is deduced by the numerical method from the equation

$$s(\lambda) = l_c - l/(\sqrt{2}\sin\gamma). \quad (22)$$

The contact pressure at the boundary EE_0 increases up to the maximal value $p_0 + 2\lambda$ at point E, where p_0 is pressure (8) at the boundary AE_0. The limiting value of angle λ constrained by the plastic yielding of the deformed protrusion's left edge is determined by the load-bearing capacity of the rigid wedge with the apex at point E

$$\lambda \le \pi/4 - \gamma + \alpha + 0.5\theta. \quad (23)$$

Udner the large values of the contact friction μ, the angle $\gamma \to 0$ and the the critical angle λ increases. The second deformation stage continues with the increase of the tool's shift Δ compared to the low values μ [9] and the residual depth of the microroughnesses' depressions.

The average normal pressure q at the boundary's contact with the tool l_c is determined by the integration of the distribution of pressure p and assumes the maximal value with the tool's finite shift Δ_0 on the exit from the deformation zone (Fig. 1). The limiting value Δ_0 is constrained by the load-bearing capacity of the plastic half-space with the sliding of a flat die with contact friction μ with the pressure limitation q by the inequality

$$q \le \pi/4 + \gamma + 0.5(1 + \sin 2\gamma), \quad \gamma = 0.5\arccos 2\mu. \quad (24)$$

RESULTS AND DISCUSSIONS

The plastic deformation of the protrusions of a rough surface has been modeled by a sliding tool using the FORTRAN programs. The programs' input data include the rough surface's parameters R_A and $2L$, the contact friction μ, the vertical shift Δ_0 of the lowest point of the tool's profile, and radius R_0 of the circular profile or the inclination angle α_0 of the linear profile.

The examples given below, with the contact friction $\mu = 0.435$ have been modeled for the parameters $R_A =$ 15 micron and $2L = 100$ micron of the rough surface to compare with the modeling results [9] with the low contact friction $\mu = 0.05$.

The inclination angles of the contact surface α and the dimensionless values of the contact boundary's vertical shift Δ, the lengths of the contact l_c, the average pressure q, and the forces Q_x and Q_y on discrete contacts with the protrusions of a rough surface and the total forces with the shift $\Delta_0 = 0.493$ (7.4 micron) for a tool with a circular arc and an inclined profile, respectively, are presented in Tables 1 and 2.

Increasing the contact friction results in a decrease of the vertical forces and an increase of the horizontal forces affecting the tool compared to the microroughnesses' plastic deformation with low contact friction values [9]. The automodeling stage of the deformation constrained by the limiting value $\Delta^* = 0.3494$ occurs in the first three protrusions of the microroughness with a deformation by a circular tool and it occurs in four protrusions with a deformation by an inclined tool.

The contact pressure, the contact boundary's length, and the force at the sixth protrusion are determined by the shift $\Delta_0 = 0.493$ with $\alpha = 0$ and they do not depend on the tool's profile.

The sliding lines of the automodeling stage of the deformation of the microroughness' protrusion for $\mu = 0.435$, $\alpha = 0.015$, $\beta = 1.279$, and $\Delta = 1/3$ (5 micron) are presented in Fig. 2. The estimated values of the angles are $\gamma = 0.2578$, $\theta = 0.2821$, and $\psi = 0.4546$. The contact pressure $p = 1.201$ and the load-bearing capacity of the rigid wedge with apex E increases in comparison with [9].

The sliding lines and the distribution of the contact pressure p at the final stage of the deformation of the sixth protrusion $\alpha = 0$ and the tool's shift Δ_0 constrained by the average pressure $q = 1.79$ of the sliding flat die on the plastic half-space are presented in Fig. 4. The final depth $\delta = 0.1345$ (2.02 micron) of the microroughness' depressions determined by the coordinates of points A and B of the stress-free boundary is considerably lower in comparison with [9].

With large values of contact friction, which can be obtained by the wear-resistant coatings' deposition on the tool's surface [4–6], the plastic regions' depth in the discrete contacts with microroughnesses decreases, verging towards the pure shift's extreme case with $\mu = 0.5$. The load-bearing capacity of the rigid region increases with the one-sided plastic shift of the material into depression δ and an improvement of the quality of the processed rough surface in comparison with the low contact friction value on the tool's surface.

Table 1. Plastic deformation of rough surface by tool with circular-arc profile with $R_0 = 20$ mm, $\mu = 0.435$

Protrusion number	α	Δ	l_c	q	Q_x	Q_y
1	0.025	0.077	0.766	1.186	0.356	0.900
2	0.020	0.227	2.268	1.194	1.040	2.686
3	0.015	0.343	3.439	1.201	1.558	4.108
4	0.010	0.427	4.410	1.260	1.974	5.537
5	0.005	0.477	5.323	1.442	2.354	7.663
6	0.000	0.493	6.006	1.776	2.613	10.660
$\Sigma Q_x = 9.894$, $\Sigma Q_y = 31.560$						

Table 2. Plastic deformation of rough surface by tool with inclined profile with $\alpha_0 = 0.125$, $\mu = 0.435$

Protrusion number	α	Δ	l_c	q	Q_x	Q_y
1	0.125	0.077	0.768	1.205	0.346	0.922
2	0.125	0.160	1.604	1.205	0.722	1.924
3	0.125	0.243	2.439	1.205	1.098	2.926
4	0.125	0.327	3.275	1.205	1.474	3.928
5	0.125	0.410	4.180	1.233	1.882	5.129
6	0.000	0.493	6.006	1.776	2.613	10.660
$\Sigma Q_x = 8.134$, $\Sigma Q_y = 25.490$						

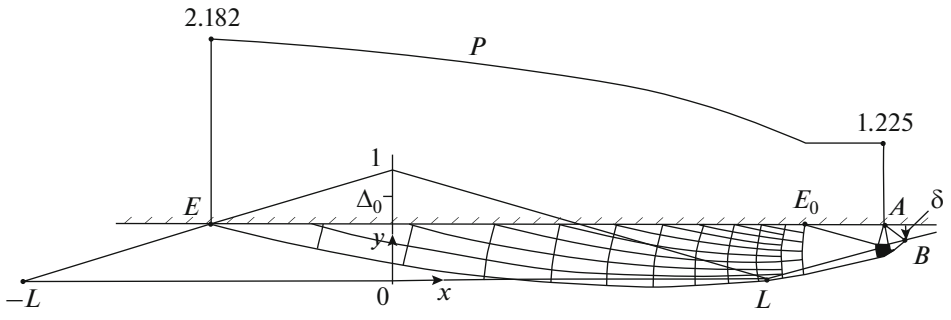

Fig. 4. Sliding lines and contact pressure at finite deformation stage with $\alpha = 0$, $\Delta_0 = 0.493$, $\mu = 0.435$.

CONCLUSIONS

The plastic deformation modeling of a rough surface with the periodic form of microroughnesses by a sliding hard tool with the high contact friction values that can be obtained by the by the depositions of wear-resistant coatings demonstrates an improvement of the quality of the processed rough surface due to the decrease of the residual depth of the microroughness' depressions with the one-sided plastic yielding of the material in the direction of the sliding of the tool.

NOTATION

R_0	radius of the tool's circular profile
α_0	inclination angle of tool's linear profile
R_A	height of microroughness, unit length
$2L$	step in protrusions and depressions of roughnesses
β	half of angle at roughness' apex
V	horizontal velocity of tool's sliding
α	angle of descent towards tool's profile at contact with roughness' protrusion
Δ	shift of vertical contact boundary in relation to roughness protrusion's apex
Δ_0	value Δ at lowest point of tool's profile
θ	plastic overflow's inclination angle towards protrusion edge
x, y	orthogonal coordinates
ξ, η	sliding lines
$2\sigma_s/\sqrt{3}$	von Mises' yield stress, stress unit
μ	dimensionless stress of Prandtl's contact friction
σ	average stress
p	normal contact pressure
φ	angle of descent towards ξ-sliding line with axis x
V_ξ, V_η	projection of velocity on sliding line
q	average pressure at contact's boundaries
ψ	angle of centered fan of sliding lines at point A
λ	angle of centered fan of sliding lines at point B
Q_x, Q_y	horizontal and vertical forces per unit length affecting tool
l	stress-free boundary length AB of plastic region with protrusions' deformation
l_c	boundary's length of protrusion contact with tool
s	contact boundaries' lengths of plastic region at interval with variable contact pressure
N_c	number of deformed protrusions at contact boundary with tool

ACKNOWLEDGMENTS

The developed programs allow us to analyze the contact loads on a tool, the surface layer's plastic deformations with the penetration depth of the order of the height of the initial microroughness and the decrease of the surface roughness depending on the form of the tool's working surface and the vertical depression of the microroughness' protrusions.

This work was supported by the Russian Ministry of Education and Science, the project no. 9.2445.2014.K.

REFERENCES

1. *Mashinostroenie. Entsiklopediya. Tom III-3. Tekhnologiya izgotovleniya detalei mashin* (Machine Engineering. Encyclopedia, Vol. III-3: Technology of Machine Parts Production), Moscow: Mashinostroenie, 2006.
2. Odintsov, L.G., *Uprochnenie i otdelka detalei poverkhnostnym plasticheskim deformirovaniem. Spravochnik* (Hardening and Finishing of Details by Surface Plastic Deformation. A Handbook), Moscow: Mashinostroenie, 1987.
3. Grechishnikov, V.A., Kolesov, N.V., and Yurasov, S.Yu., Roughness in cylindrical milling, *Vestn. Mosk. Gos. Tekh. Univ., Stankin*, 2012, no. 4 (23), pp. 49–50.
4. Grigoriev, S.N., Romanov, R.I., and Fominskii, V.Yu., Dependence of mechanical and tribological properties of diamond-like carbon coatings on laser deposition conditions and alloying by metals, *J. Frict. Wear*, 2012, vol. 33, no. 4, pp. 253–259.
5. Grigorev, S.N., Kovalev, O.B., Kuzmin, V.I., Mikhal'chenko, A.A., Rudenskaya, N.A., Sokolova, N.G., and Fomin, V.M., New possibilities of plasma spraying of wear-resistant coatings, *J. Frict. Wear*, 2013, vol. 34, no. 3, pp. 161–165.
6. Antonenkova, G.V. and Chubarov, S.V., Analysis of the surface wear-resistant layer formed using vacuum-arc discharge plasma, *Vestn. Mosk. Gos. Tekh. Univ., Stankin*, 2012, no. 4 (23), pp. 73–77.
7. Ishlinskii, A.Yu. and Ivalev, D.D., *Matematicheskaya teoriya plastichnosti* (Mathematical Theory of Plasticity), Moscow: Fizmatlit, 2001.
8. Nepershin, R.I., Plastic deformation of surface layer during rigid cylinder rolling and sliding, *J. Frict. Wear*, 2013, vol. 34, no. 3, pp. 204–207.
9. Nepershin, R.I., Plastic deformation of rough surface by a sliding tool, *J. Frict. Wear*, 2015, vol. 36, no. 4, pp. 293–300.
10. Nepershin, R.I., *Applied Problems of Plasticity*, Moscow: MSTU "STANKIN", 2016.

Translated by V. Melnikov